GRC Transactions, Vol. 47, 2023

Integrated Conceptual Model of Sedimentary Basin-Hosted Geothermal Fields in Imperial Valley, CA

Gabrielle Ramirez, Robin Zuza, Adam Johnson, John Murphy and John Akerley

Ormat Technologies, Inc.

Keywords

conceptual model, sedimentary basin, rift basin, matrix permeability, Imperial Valley, Salton Trough

ABSTRACT

Imperial Valley, CA generates up to 720 MW[1] of renewable energy from geothermal power plants and Ormat Technologies, Inc. successfully operates 3 out of 4 of the contributing geothermal complexes: Heber, Brawley, and Ormesa. These fields, along with the Salton Sea Geothermal Field, are situated in the Salton Trough, a tectonically active pull-apart basin that occurs at a major step in the San Andreas Fault System and forms a continental rift zone between the Pacific and North American plates. The Salton Trough has anomalously high heat flow attributed to crustal thinning and magmatic intrusions as well as extensive faulting related to rifting. While sedimentary basins have been a focus for geothermal globally, the Salton Trough is unique due to the relatively shallow depths to thick sequences of hot, clastic sediments. Heber, Brawley, and Ormesa geothermal fields are moderate to low temperature resources primarily hosted in high-porosity sediments and highly influenced by rift-related fault and fracture networks. Although there are similarities in resource temperatures and depths between Ormat fields, there are key differences in permeability distribution. To characterize reservoir properties (e.g., porosity, net reservoir, grain size and sorting, compartmentalization, and fracture permeability) and ensure best practices in reservoir management, it is critical to integrate petrophysical logs, production logs, and 2D/3D seismic data sets where available. We use data from key wells in each of the Ormat-operated geothermal fields to understand how paleo-environment of deposition and faulting control permeability and create data-driven and fully integrated conceptual models.

[1]California Energy Commission, California Geothermal Energy Statistics and Data (2020)

1. Introduction

Sedimentary basins are recognized worldwide as an opportunity to expand both conventional and enhanced geothermal energy production as demand for renewable sources grows. Prospective sedimentary basins must have sufficient temperature, thickness, porosity, and permeability occurring at depths that are economically feasible to drill (Anderson, 2013). The successfully operated geothermal fields in the Imperial Valley present a unique opportunity to study conventional sedimentary basin-hosted geothermal systems due to the presence of anomalously high heat flow and thick sequences of clastic, high-porosity sediments at relatively shallow depths.

Ormat Technologies, Inc. operates 3 geothermal fields in the Imperial Valley with a combined generating capacity of 130 MW. These include the Heber, Brawley, and Ormesa complexes (Figure 1). All three currently produce pumped, single-phase fluids using binary technology. Ormesa, Heber, and Brawley were initially developed in 1976, 1982, and 2009, respectively. Heber and Ormesa were among the first binary projects in the US.

These three fields are situated in the Salton Trough which has anomalously high heat flow attributed to crustal thinning and magmatic intrusions as well as extensive faulting related to rifting. Heber, Ormesa, and Brawley geothermal fields are primarily hosted in high-porosity sediments and are strongly influenced by rift-related fault and fracture networks. Extensive data from these fields present an opportunity to explore the interplay between matrix and fracture permeability within successfully operated conventional geothermal systems. After reviewing the overall geological context of all three fields, we review the implications of geochemistry, temperature patterns, and controls on permeability for each field in turn before presenting their integrated conceptual models.

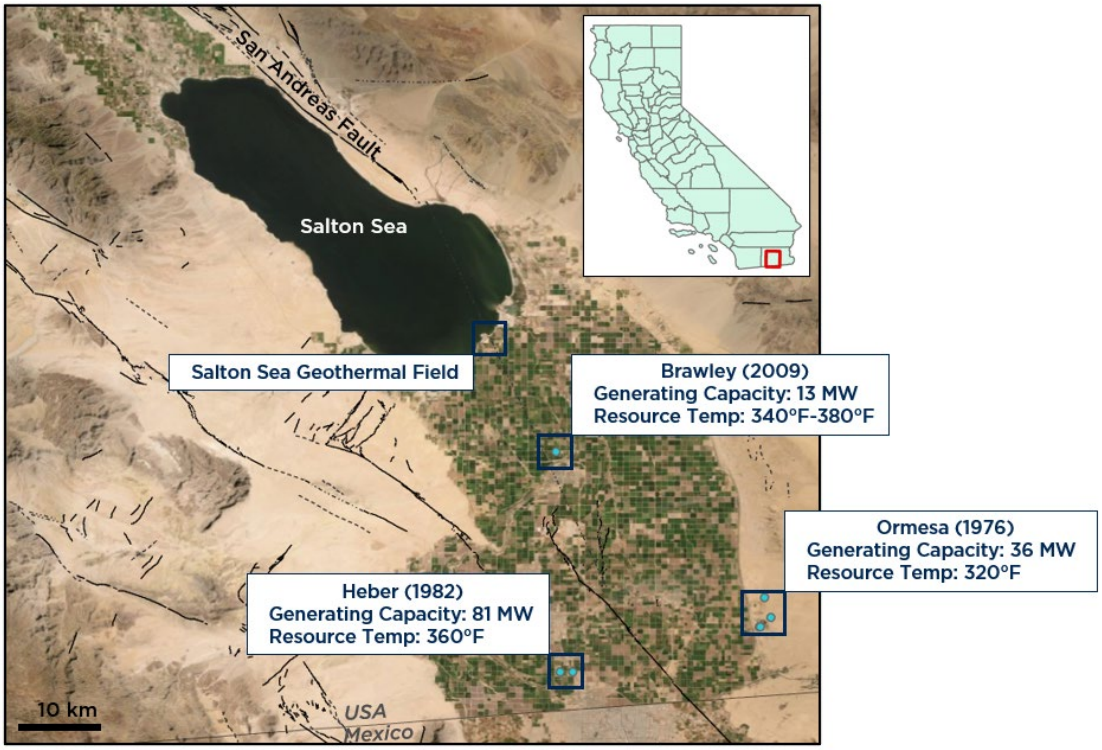

Figure 1: Ormat-operated fields and Salton Sea Geothermal Field in the Imperial Valley, CA with the year the power plant came online, current generating capacity, and resource temperature. Base map is Google Earth imagery overlaid with USGS Quaternary faults.

2. Geologic Setting

The Ormat-operated geothermal fields reside in the Salton Trough, a tectonically active pull-apart basin that occurs at a major step in the San Andreas Fault system forming a continental rift zone between the Pacific and North American plates (Figure 2). Within this rift zone, there are a series of smaller-scale pull-apart basins bounded by northwest-trending strike-slip faults and northeast-trending normal faults that accommodate extension. The Salton Trough has anomalously high heat flow of greater than 100 mW/m^2 attributed to both crustal thinning and deep magmatic intrusions (Sass et al., 1984). Seismic imaging in the Salton Trough indicates a crustal thickness of 17-18 km (Han et al., 2016) compared to typical continental crust thickness of 30-70 km (Mooney et al., 1998). The Ormat-operated fields have locally high heat flows of >300 mW/m^2 due to conductive heat transfer and localized upwelling of hydrothermal fluids. Higher heat flows of >500 mW/m^2 are concentrated near modern-day Salton Sea and Salton Sea Geothermal Field due to Quaternary volcanism (Sass et al., 1984).

Deformation related to right-lateral motion of the San Andreas Fault resulted in extension, transtension, and crustal subsidence creating increased accommodation space for deposition of thick sedimentary sequences during the Miocene through the Pleistocene (Dibblee, 1954, 1984; Johnson et al., 1983; Winker, 1987; Herzig et al., 1988; Winker and Kidwell, 1996). Moderate basin subsidence in the Miocene led to the deposition of coarse-grained conglomerates and alluvial fans, referred to as the Split Mountain Group, lying unconformably on Mesozoic granitic basement. A marine incursion in the Late Miocene from the Gulf of California filled the Trough with marine shales and turbidites known as the Imperial Group (Figure 3a). Following the marine incursion, the Colorado River deposited a large volume of sediments from the northeast into the Salton Trough during a period of rapid subsidence (Dorsey et al., 2011). This resulted in the progradation of the fluvial delta plain into the northern end of the Gulf of California and filling of the Trough up to sea level with the Palm Springs Formation (Figure 3b). The Palm Springs Formation is characterized by avulsing channels, flood plains, and ephemeral lakes and provides the high-porosity sediments that host the Ormat-operated geothermal systems. The Colorado River exit point into the rift basin at approximately 4 Ma was at the intersection with the San Andreas Fault north of present-day Salton Sea (Figure 3b). Over the next 2 million years, the right lateral motion of the San Andreas Fault moved the exit point to the southeast along the fault and south of present-day Salton Sea (Figure 3c). The lateral equivalent of the upper Palm Springs Formation is the Borrego Formation which is composed of mudstone and claystone deposited by a paleo-lake in the Trough to the north of the Colorado River deposition. As the exit point of the Colorado River migrated to the southeast along the San Andreas Fault, the deposition of the Borrego Formation sediments expanded to the southeast capping the Palm Springs Formation. Overlying the Palm Springs and Borrego Formations is the mudstone- and claystone-rich Brawley Formation that also serves as an impermeable cap to the geothermal fluids (Kirby et al., 2007). The sedimentary sequences are typically greater than 4 km thick in the Trough (Figure 4).

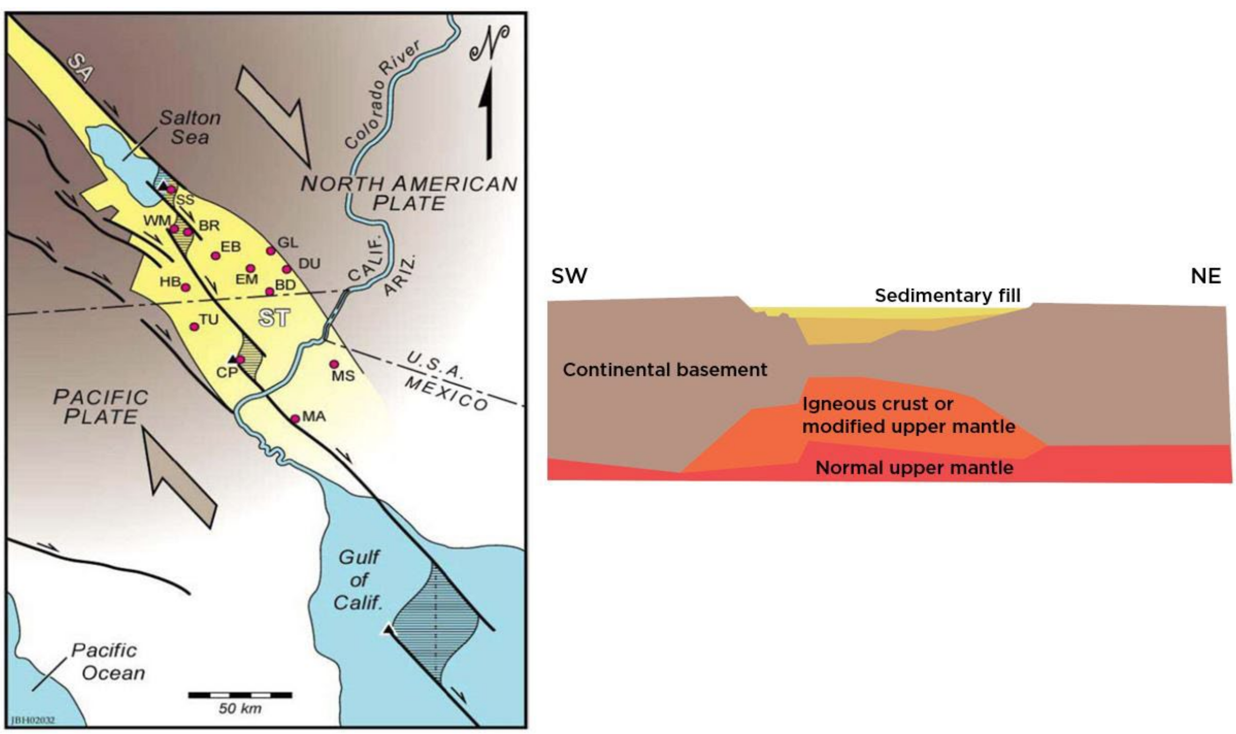

Figure 2: (Left) Location and tectonic map of the Salton Tough (ST) and geothermal systems from Kaspereit et al., 2016 (HB=Heber, BR=Brawley, and EM=Ormesa). (Right) Schematic x-section through the Salton Trough based on gravity and seismic refraction data showing anomalously thin crust below the basin (modified from Lonsdale, 1989).

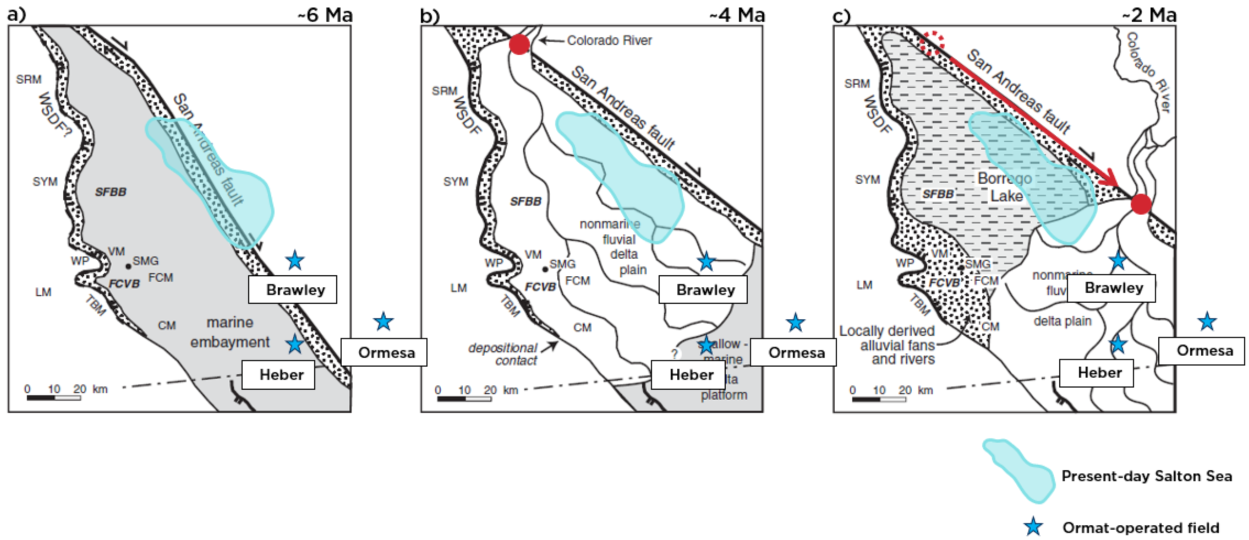

Figure 3: Paleogeographic reconstructions of the Salton Trough and surrounding region at 6, 4, and 2 Ma modified from Dorsey et al., 2011 with present-day locations of Heber, Brawley, Ormesa, and the Salton Sea. a) Moderate subsidence and a marine incursion in the Late Miocene (~6 Ma) led to the deposition of the coarse-grained Split Mountain Group and the marine shale- and turbidite- dominated Imperial Group on top of Mesozoic granitic basement. b) During a period of rapid subsidence in the Pliocene (~4 Ma), progradation of the of Colorado River and delta into the Salton Trough deposited the high-porosity sands of the Palm Springs Formation, the primary reservoir formation for Heber, Brawley, and Ormesa geothermal fields. The exit point of the Colorado River and delta at this time is marked by the red dot. c) By the early Pleistocene (~2 Ma), the right lateral motion of the San Andreas Fault moved the exit point and depositional center of the Colorado River and delta to the southeast. As a result, mudstone and claystone were deposited by Borrego Lake and, as the exit point continued to migrate to the southeast along the San Andreas Fault, these fine-grained sediments capped the high-porosity Palm Springs Formation. The mudstone- and claystone- rich Brawley Formation, which overlies the Palm Springs and Borrego Formations, also serves as an impermeable cap, inhibiting the flow of geothermal fluids to the surface.

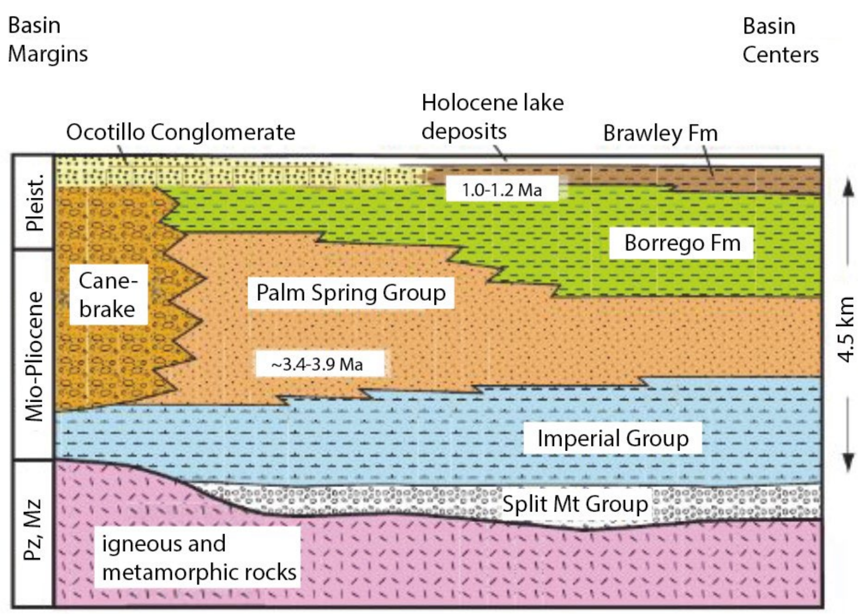

Figure 4: Simplified stratigraphic section of the Salton Trough modified from Lutz et al., 2006.

3. Geochemistry

Extensive geochemical studies exist for the individual geothermal systems hosted in the Salton Trough, with most studies having focused on the hypersaline brines produced from the Salton Sea Geothermal System and its Cierro Prieto counterpart to the south. These studies have largely focused on the origins of hypersaline brines in the Salton Sea and the degree of magmatic influence on the system. Overall, geothermal brines in the Salton Trough are controlled by a continental, evaporative salt signature where freshwater lakes that formed during the flow of the Colorado River into the closed basin gave rise to ancestral hypersaline lacustrine systems. This contrasts with the more marine salt signature in the south where mixing between the deltaic Colorado River and hydrothermally altered seawater dominates at Cierro Prieto (Elders, et al., 1974; Elders, et al., 1983; Lippman, 1999). The high metal contents found in the Salton Sea fields are likely leached from Colorado River deltaic sediments during high-temperature water-rock interactions (Doe, 1966; White 1981), although sources of sulfur in the system may be derived from either primary magmatic activity or as detrital sulfides from weathering of igneous provinces (White, 1981). Evidence for magmatic input associated with Quaternary continental volcanism is seen in higher temperature systems, such as Salton Sea and Cierro Prieto, and based on elevated He isotopic ratios ($R/Ra > 6$) and carbon isotopic values of CO_2 (Elders, 1983; Mazzini, 2011). Moderate to low temperature systems, such as Heber, Brawley, and Ormesa, do not show this mantle-derived input and are attributed solely to the high heat flows in the area from crustal thinning (Elders, 1983). Vertical changes in salinity in the Salton Sea have been attributed to density differences and the perching of a less saline geothermal fluid over dense, hypersaline brines with over 20% total dissolved solids (TDS). This density interface crosscuts sedimentary features and bedding planes (Williams, McKibben 1989).

3.1 Brawley

The most northern of the operating Ormat facilities hosts a slightly acidic, brackish sodium-chloride fluid with a TDS content of up to 14,000 mg/L. Minor brine constituents include elevated levels of boron and magnesium, which are an order of magnitude higher than those seen in either Heber or Ormesa. The resource has the highest reported gas content of the Ormat facilities, reaching nearly 0.7 wt% of largely CO_2 (> 99%) with trace amounts of H_2S and N_2/Ar ratios that are expected for air-saturated water (N_2/Ar =52-56). Methane values range from 12-29 ppm in the fluids and likely represent high-temperature water-rock interactions with organic-rich lacustrine sediments which is consistent with the elevated metals and boron in the system. High gas content may also be due to high-temperature alteration of organic-rich lacustrine sediments to thermogenic gas. While lateral variability in the system is likely controlled by stratigraphy, vertical variability is controlled through density stratification like what is seen in the Salton Sea geothermal field (Williams, McKibben, 1989). Deeper hypersaline fluids have been encountered in several exploration drilling wells in the late 1970’s with TDS above 200,000 mg/L and chemical compositions similar to Salton Sea brines. Because these deeper fluids caused corrosion and severe scaling problems, Ormat has focused development on the shallower, lower temperature resource (<4000ft depth).

3.2 Heber

The Heber complex contains similarly slightly acidic, brackish sodium-chloride brine as seen at Brawley, with a slightly lower range of dissolved solids of 10,000-12,000 mg/L. A high amount of calcium in the fluids, over 900 mg/L, buffers gas concentrations which are significantly lower (0.02-0.05 wt%) than Brawley and consist of 80-90% CO2 with minor amounts of methane and N2/Ar ratios consistent with air-saturated water (N2/Ar-39-42). Compositional differences between Heber and Brawley are likely associated with the degree of high-temperature interactions between brine and lacustrine sediments. Heber has lower metal content, lower boron, and reduced methane concentrations which indicates lower lacustrine input compared to Brawley. Heber fluids have been characterized as residual brines from ancestral Lake Cahuilla (Rex, 1983) and show Cl/Br ranges of 900-1150 compared to Colorado River Cl/Br values of 1600 and Cl/Br values of over 20,000 from hypersaline brines. This is consistent with Heber's position within Lake Cahuilla maximum extent during deposition. The high calcium content may originate from gypsum deposition in ancestral Lake Cahuilla.

3.3 Ormesa

Ormesa contains three individual plants producing two distinct fluid types. The northern Ormesa 1 (O1) facility generates a neutral dilute sodium-chloride-bicarbonate brine with a TDS of less than 2,000 mg/L. Gas concentrations in these fluids range from 0.09-0.14 wt% and over 94% CO_2. Both nitrogen and methane show wide ranges of variability, between 2 and 4 mole percent nitrogen and 0.7 to 2.5 mole percent methane, with N_2/Ar ratios consistent with air saturated water (N_2/Ar =32-33). Cl/Br ratios for the O1 brines range from 950-1200 and suggest a similar salt source as the Heber fluids (ancestral Lake Cahuilla) but the low salinity of these fluids and the low N_2/Ar ratios may be due to recent dilution by local precipitation (Rex, 1983). Ormesa 2 (O2) and Ormesa 3 (O3) produce a neutral sodium-chloride brine with TDS values of 4800-5300 mg/L. O2 has a higher and wider range of gas content (0.07 to 0.18 wt%) and composition compared to O3 which shows a narrow range of gas concentrations (0.10 to 0.11 wt%) of primarily CO_2. N_2/Ar ratios for O2 and O3 range between 35-39 and suggest that variability in gas composition is likely attributed to the extent of high-temperature alteration of lacustrine shales and mudstones. Cl/Br ratios for Ormesa 2 and 3 are variable and range from 1200-1500, closer to the Cl/Br ratio of Colorado River water and suggesting the source of salt in this portion of the field may be less controlled by halite deposition in ancestral Lake Cahuilla and more with evaporative processes from the Colorado River. The mixed salt source at Ormesa is consistent with the position of the field on the border of the maximum extent of Lake Cahuilla and more adjacent to the source of the Colorado River in the east compared to the other fields.

4. Temperature

The Ormat-operated fields are low to moderate temperature geothermal systems with resource temperatures ranging between 320°F and 380°F although upflow temperatures can be as high as 500°F. Resource temperature in this context refers to the temperature that is closest to upflow fluids coming from deeper basement structures and flowing into the overlying sediment packages being actively produced by Ormat. Individual well production temperatures vary depending on location in the field and elevation of the feed zone. While portions of the Ormesa and Heber complexes produced two-phase fluids historically, there have been a number of binary expansions and repowers to increase generation, and all the wells are currently pumped. This allows for several benefits to reservoir management including, increasing well outputs, flexibility in operating parameters, preventing well scaling, simplified facilities, and easier monitoring.

The shape of the isotherms for a geothermal system is directly related to geologic factors that control the geometry of the permeable reservoir (Wallis et al, 2017). In fault-hosted systems, reservoir permeability is localized within discrete, dilated fractures, and this results in focused upflow of geothermal fluids and narrower isotherms. In sedimentary basin-hosted systems, there is a broader distribution of permeability through vertically stacked and laterally extensive high-porosity sediments which results in less constrained upflow and broader outflow plumes. Temperature profiles of productive wells in these systems can be conductive, isothermal, or mixed depending on proximity to vertical permeability (Figure 5). Fault-hosted systems will have a narrower range of temperatures while sedimentary basin-hosted systems will have a larger range of temperatures for an individual field that can be produced.

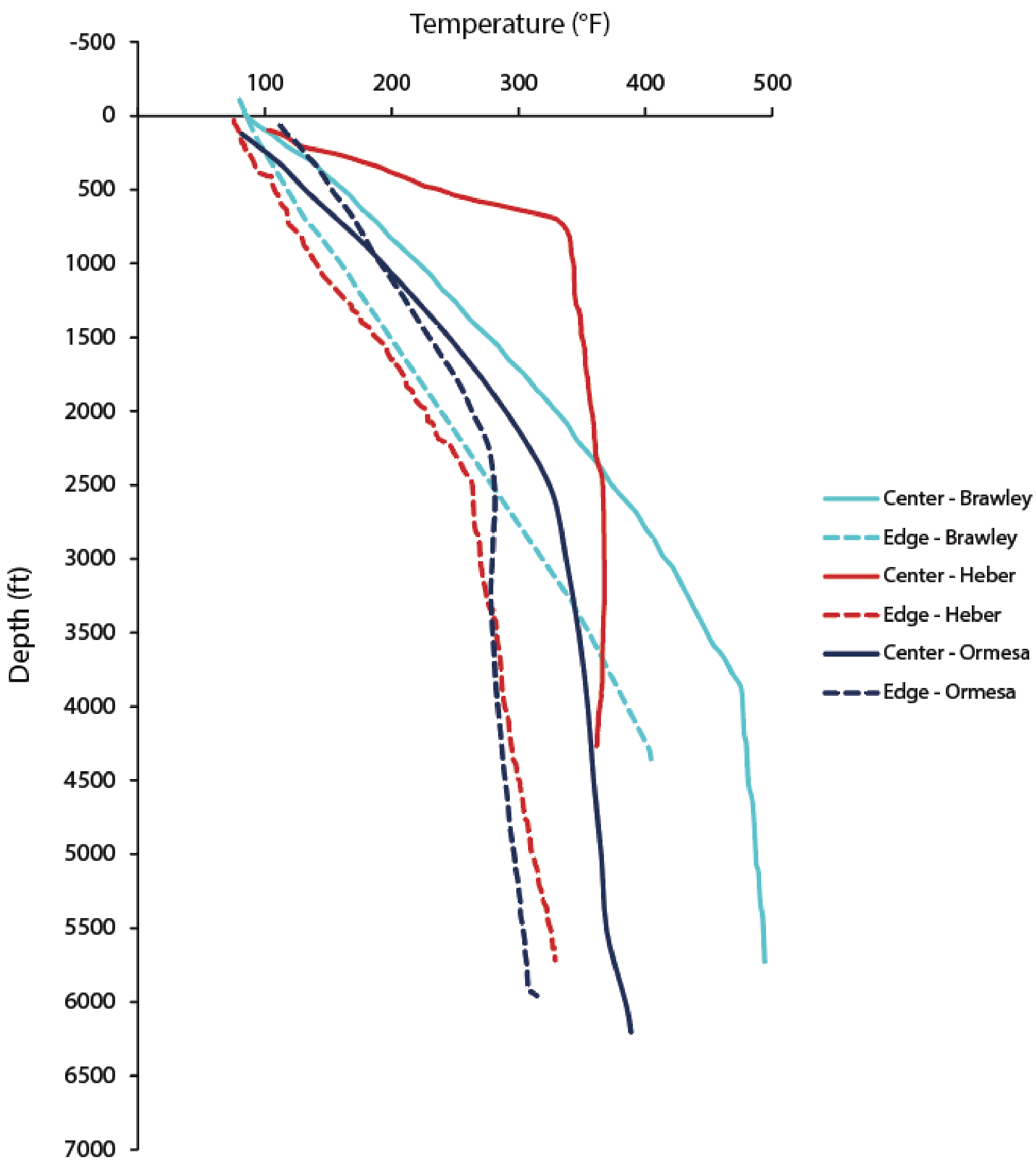

Figure 5: Temperature profiles from wells at the center and on the edge of Heber, Brawley, and Ormesa geothermal fields. Profiles can be conductive, isothermal, or mixed depending on proximity to upflow.

4.1 Brawley

The upflow temperature for Brawley is 500°F in the deeper, hypersaline reservoir (>4000ft depth). The reservoir sands that are produced by Ormat shallower than 4000ft depth are conductively heated by the upflow resulting in resource temperatures of 340°F in North Brawley and up to 380°F in East Brawley (Figure 5, 6a). These two sides of the field are considered to not be in pressure communication due to faults creating impermeable barriers and compartmentalization in the subsurface reservoir and therefore have separate production and injection configurations. Initial exploration in the 1970's targeted the deeper and hotter upflow greater than 4000ft below ground level. This deeper reservoir is dominated by fracture permeability and can be considered the root of geothermal system and convective upflow which is consistent with isothermal temperature profiles at these depths (Figure 5). The hypersaline brines at these depths were highly corrosive and presented major scaling challenges. Ormat's development strategy focused on the shallower, moderate temperature reservoir within high permeability sedimentary sequences.

4.2 Heber

The upflow and resource temperature for Heber is 360°F. Temperature profiles in the center of the field are isothermal below the clay cap of the Borrego-Brawley Formations, with production wells targeting the upflow and well production temperatures varying depending on feed zone depth and location in the field. Upflow of 360°F fluids is elongated in the NNE orientation controlled by a fracture zone (Figure 6b). The Heber 2 wellfield have conductive profiles that steepen with depth (Figure 5). They delineate the asymmetrical outflow plume emanating from the NNE fracture zone. The outflow preferentially flows to the west and northwest and is limited to the east. The current conceptual model considers this is an effect of anisotropy of reservoir quality as well as the influence of groundwater movement in this direction. High shallow temperature gradients range from 10-30°F/100ft and static temperatures >300° occur at 500ft below sea level. The Heber field has higher temperatures at shallower depths compared to Brawley and Ormesa because the Heber fracture zone extends up to a shallower depth.

4.3 Ormesa

The resource temperature for Ormesa is 320°F and the deeper upflow temperature is most likely greater than 380°F. Upflow is concentrated in the south between O2 and O3 with an asymmetric outflow to the north influenced by the presence of good reservoir quality sands (Figure 6c). The higher production temperatures in the southern part of the field coincide with the approximate location of the hinge of the central Ormesa anticline and a deeply rooted fault interpreted to core the anticline. This may be evidence that structure plays a first-order control on upflow and temperature distribution in the Ormesa field. Temperature profiles in the field are primarily conductive with a gradient change related to stratigraphic boundaries. Generally, the profiles have near-isothermal gradients in the high-porosity sands of the Palm Springs Formation and conductive gradients in the low-porosity clay cap of the Borrego-Brawley Formations (Figure 5).

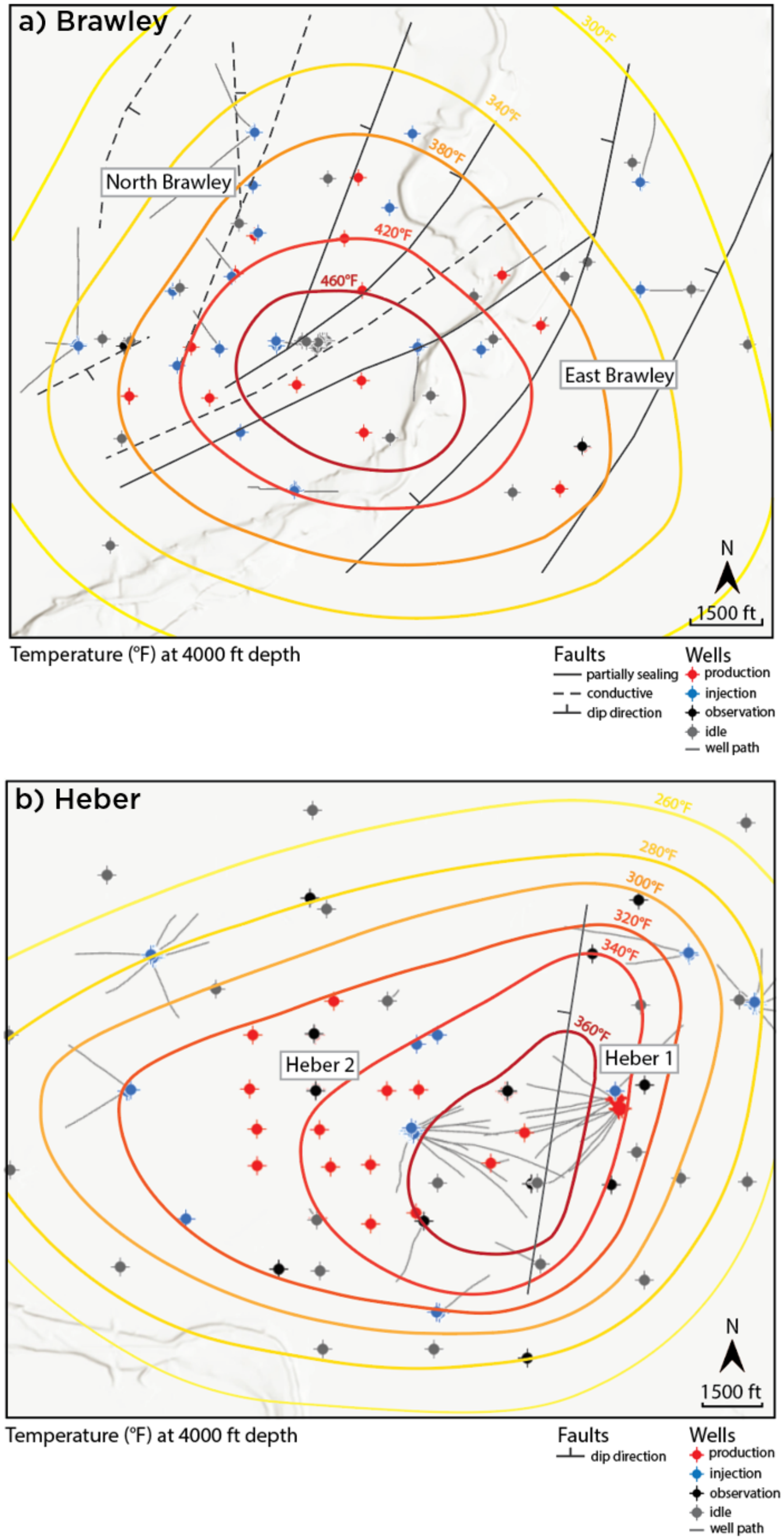
a) Brawley
300°F
340°F
380°F
420°F
460°F
North Brawley
East Brawley
N
1500 ft
Temperature (°F) at 4000 ft depth
Faults
partially sealing
conductive
dip direction
Wells
production
injection
observation
idle
well path
b) Heber
260°F
280°F
300°F
320°F
340°F
360°F
Heber 2
Heber 1
N
1500 ft
Temperature (°F) at 4000 ft depth
Faults
dip direction
Wells
production
injection
observation
idle
well path

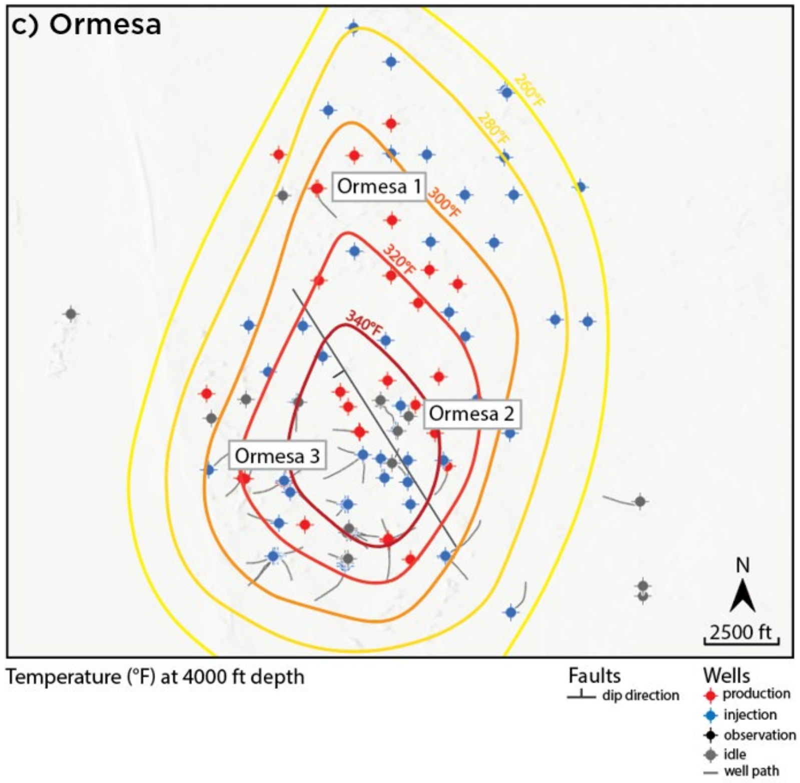

Figure 6: Temperature isotherms derived from natural state models at 4000ft below ground level for a) Brawley, b) Heber, and c) Ormesa geothermal fields. Map also includes location of production injection, observation, and idle wells with well paths. Major faults are delineated with a tick mark in the direction of dip.

5. Permeability Controls: High-Porosity Sands and Fractures

The distribution of permeability at Heber, Brawley, and Ormesa is primarily controlled by the distribution and characteristics of clastic sediments from Colorado River-derived sands with a secondary influence of fractures related to rifting. Stratigraphic controls on effective permeability include the lateral continuity of avulsing channel deposits, grain size, rounding, and sorting. Methods used to characterize the distribution of matrix permeability in sedimentary basin-hosted geothermal systems include petrophysical logs, such as gamma ray and density-porosity, and lithologic data from mudlogs. Gamma ray (GR) logs measure the natural radioactivity in formations intersected by the borehole and are used for identifying and correlating lithologies. Sandstones have lower concentrations of radioactive material than shale-rich rock and therefore give lower GR values. Density-porosity (DPHI) logs calculate the porosity along a borehole by using a density log and assuming the matrix and fluid densities.

Using downhole log data, we identify potentially permeable reservoir rock by applying cutoff values of < 80 API for GR and > 24% porosity as observed by DPHI. The rock that meets this criterion we deem “Net Reservoir” (NR). These cut offs are useful to identify potential flow units and have been calibrated against production and PTS (Pressure, Temperature, and Spinner) logs. Figure 7 serves as an example from a perforated Heber injection well of how feed zones interpreted from spinner data correlate with stacked intervals of high net reservoir, net-to-gross (NTG), and maximum bed thickness. The largest contributing feed zone is indicated by the inflection in spinner data from 3200 to 3500ft and correlates to an interval with high net reservoir, the largest values of NTG, and the largest maximum bed thickness. Although the correlation between interpreted feed zones and reservoir characteristics is clear for the majority of the perforated section of the well, there is a zone between 5000 and 5700ft with multiple intervals of net reservoir that do not correlate with an interpreted feed zone in the spinner data. While net reservoir may be present, other factors such as alteration and the geometry of the sand packages must be taken into account. From 5000 to 5200ft, mudlog data indicates common to abundant chlorite alteration. The presence of clay minerals, such as chlorite, reduces pore throat size (or the narrow channel between pore spaces) and overall permeability in sandstones (Ahmad et al., 2018). From 5200 to 5700ft, the thickness column shows unstacked, thin beds of net reservoir. Mudlog data supports this by indicating a high degree of interbedded claystone over this interval. The geometry of unstacked, thin sands reduces vertical and lateral continuity and increases the chance of compartmentalization, making this interval a poor candidate for a meaningful feed zone.

While matrix permeability from high-porosity clastic sequences is the primary form of permeability for Ormat-operated fields, fracture permeability is also present to varying degrees. Methods used to characterize the presence of fracture permeability include drilling data (i.e., loss circulation), borehole image logs, dipmeter logs, and 2D/3D seismic reflection data. The methods mentioned above will be used to describe matrix and fracture permeability distribution in each of the Ormat-operated fields.

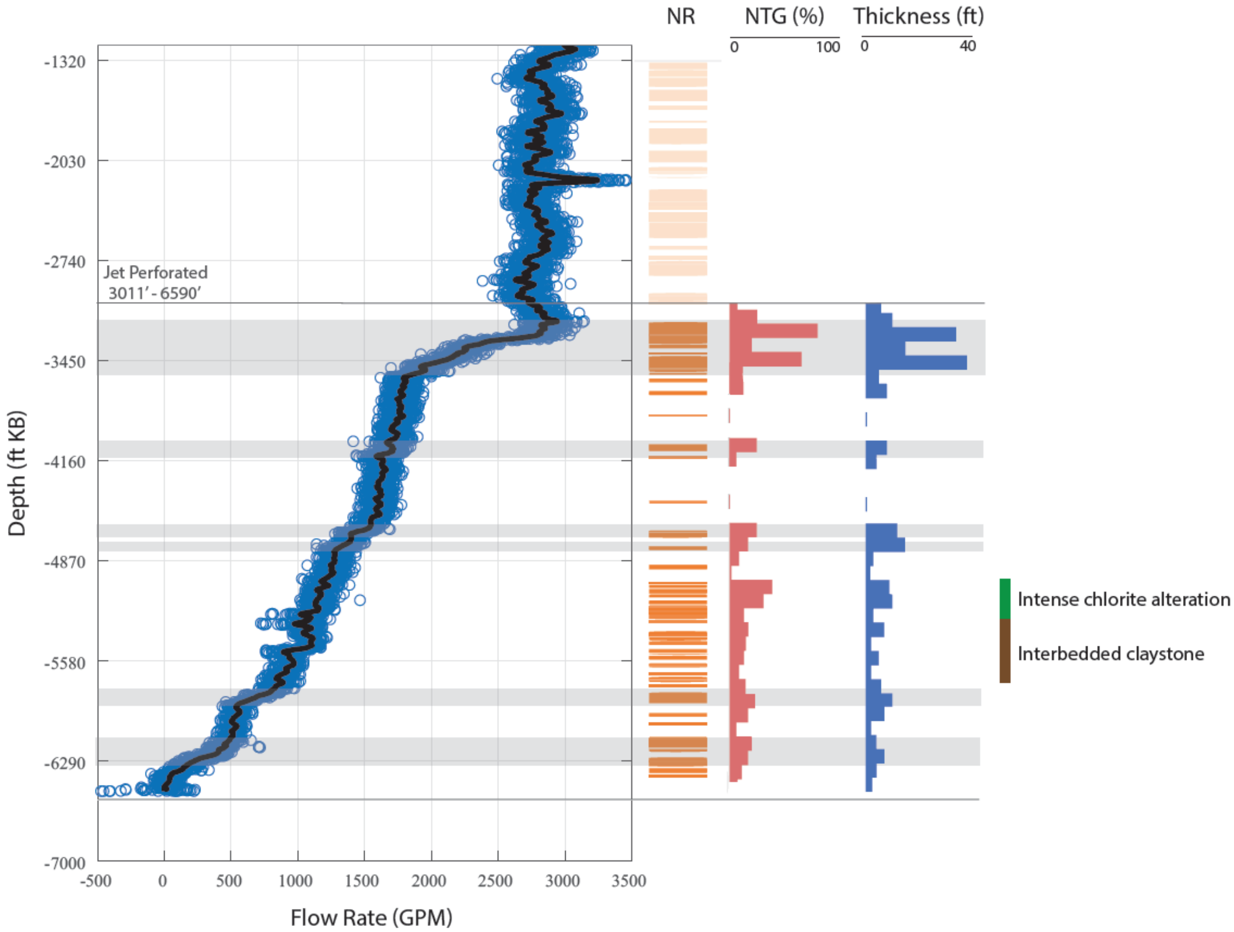

Figure 7: Flow rate calculated from spinner data for a perforated injection well at Heber. Columns next to the flow rate data include net reservoir (NR), net-to-gross (NTG), and maximum bed thickness. Shaded gray boxes are interpreted feed zones from spinner data. Interpreted feed zones correlate to stacked intervals of high net reservoir, NTG, and maximum bed thickness. Factors such as alteration and the geometry of the sand packages can explain the lack of interpreted feed zones over high net reservoir intervals.

5.1 Brawley

Primary permeability of the shallow Brawley reservoir is mainly attributed to clastic sequences between 2000 and 4000ft below sea level within high-porosity Palm Springs formation clastic sediments. This is evidenced from electric logs, production logs, and mud logs. Siltstone and claystone units are interbedded with moderately thick (50-75ft), very fine to fine, well-rounded, and well-sorted sands (Figure 8). Production and injection feed zones, or intervals that are proven to be permeable enough for fluid flow through well testing, correspond to intervals of high-porosity sand intervals between 2000-4000ft in Brawley. There is a large reduction in reservoir quality deeper than 4000ft below surface attributed to diagenetic compaction, hydrothermal mineralization, and increased clay-content reducing effective permeability (Figure 9). Net reservoir thickness also varies laterally in the field with increasing net reservoir from east to west. This is attributed to packages of growth strata in the hanging wall of northeast-trending normal faults increasing the sand content in the North Brawley region. Above the main flow units from surface to 2000ft depth, the lithology is dominated by thick claystone units with thin interbedded sands including layers of anhydrite and gastropods, most likely from perennial lake deposits of the capping Borrego Formation. Overall, the Brawley geothermal field shows a greater degree of sand-poor (GR>80, DPHI<24%) layers and a rapid reduction in net reservoir with depth compared to Heber and Ormesa. This is most likely due to a greater degree of lacustrine deposition with Brawley's position in the center and lowest part of the rift basin. Additionally major flow units between 2000 and 4000ft are not laterally continuous and electric log correlation suggests fast lateral changes in facies consistent with a dynamic fluvial-deltaic environment of deposition.

Multiple wells have encountered fracture permeability in the deeper Brawley reservoir below 4000ft depth. Fracture permeability at Brawley is evidenced by lost circulation zones, image and production logs and typically associated with higher-than-average well productivity or injectivity. Mud log data over some fracture zones also showed an increase in quartz veining as well as euhedral quartz, suggesting mineralization was occurring in open, permeable fractures. Fracture orientations measured from image logs in Well A and B have a dominant strike of N15°E and which is consistent with fault orientations mapped in the Brawley 3D seismic survey. Well C, seen in Figure 10a, was drilled in the center of the field and closest to the inferred upflow. The well encountered total loss circulation at a fracture at 4500ft depth. This zone was permeable but produced a highly corrosive, hypersaline fluid with a TDS of ~100,000 mg/L at 489°F. Due to the corrosivity of the deeper hypersaline fluid, the decision was made to seal off the fracture zone. To further explore the nature of faulting in Brawley, Ormat acquired a 3D seismic survey covering 9.5 square miles in 2011. The survey was very successful at mapping high angle fractures throughout the field along with both continuous and discontinuous reflectors supporting the stratigraphic controls on permeability distribution. An updated structural model was derived with this dataset using numerous seismic processing techniques and attribute mapping. The structural model supported the expected fault configuration with NNE to ENE striking normal faults related to the Brawley Fault Zone. Tracer studies in the Brawley field have shown that some of these faults are conductive while others impede fluid flow and do not allow for pressure communication with adjacent fault blocks, such as the fault between North Brawley and East Brawley. The Brawley 3D seismic volume led to the discovery of a poor reflectivity zone (PRZ), an area of chaotic reflectors and poor seismic image quality within the deeper reservoir. A PRZ is hypothesized to occur when densification of sediments due to hydrothermal mineralization lowers impedance contrast between stratigraphic layers. Although the image is too poor to show discrete faults, the presence of a PRZ can be evidence of the root of the geothermal system or upflow that drives the conductive heating of the above sediments.

5.2 Heber

Primary permeability in Heber is attributed to clastic sequences of the Palm Springs Formation as well as NNE-oriented fracture zones between 2000 and 8000ft depth. Electric logs and mud logs show thick (>100ft) layers of high to moderate porosity, very fine to fine, well-rounded, well-sorted sands interlayered with thin siltstone layers (Figure 8). Compared to Brawley, Heber has a milder reduction in net reservoir deeper than 4000ft indicative of a longer residence time in the depositional center of Colorado River deposition (Figure 9). Net reservoir increases from east to west, with thicker net reservoir in the Heber 2 wellfield. This is most likely related to temperature-dependent processes, such as cementation, being more prevalent in the higher temperature Heber 1 wellfield. Above the main flow units from surface to 2000 ft depth, the lithology is dominated by 100-200ft thick claystone interbedded with thin sand lenses. These clay-rich sections are the Borrego-Brawley Formations that provide the caprock to the geothermal system.

Below 4000ft, there is evidence for fractures in indurated, moderate to low porosity sandstones of the Palm Springs Formation. For example, Well A has multiple lines of evidence for a fracture zone including total loss circulation while drilling, a dramatic steepening of dips seen in a dipmeter log, and an image log of a large aperture fracture. The static temperature profile for Well A also becomes isothermal at the depth the fracture was intersected, indicating the fracture is a permeable conduit for convective fluid flow. At a similar depth, nearby Well B has similar evidence for a fracture zone as well as pressure, temperature, and spinner data suggesting the fracture zone provides the majority of production for the well. The fracture zone intersected by Well A and Well B, along with other wells in the center of the field, trends approximately N10°E and is steeply dipping (Figure 10b). The trend of the fracture zone is corroborated by the narrowing trend of the temperature isotherms as well as legacy 2D seismic line. The 2D seismic shows a PRZ at the approximate location of the fracture zone, indicating densification of sediments due to hydrothermal mineralization from focused geothermal fluid flow similar to the deeper section in Brawley.

5.3 Ormesa

Primary permeability in Ormesa is attributed to clastic sequences of the Palm Springs Formation between 2000 and 6000ft depth (Figure 8). Electric logs and mudlogs show a greater amount of net reservoir compared to Heber and Brawley that consists of thick (>100ft), medium to coarse, sub-rounded to angular, and poorly sorted sands (Figure 9). This contrasts with well-rounded, very fine to fine sands with good sorting encountered at Heber and Brawley and is consistent with Ormesa being the most proximal field to the exit point of the Colorado River at the eastern edge of the basin. The northern part of the Ormesa field has higher net reservoir values than the south and this most likely influences the direction of the broad outflow to the north. Above the main flow zone units from surface to 2000ft depth, the caprock formation consists of thick (>50ft) interbedded claystone and thin sands. The proximity of Ormesa to the source of Colorado River sediments increases the amount of net reservoir but may also lower effective permeability due to poor sorting and angularity of sand grains.

There is evidence for fracture zones below 6000ft in drilling data and legacy 2D seismic. Well A in Figure 10c encountered total loss circulation, drilling breaks, and euhedral quartz that correlate with slightly shallower total loss circulation zone encountered in Well B. This would correspond to a steeply dipping fault dipping to the southwest located in the hottest part of the field. Legacy 2D seismic data shows a PRZ in the approximate location of the steeply dipping fault seen in Well A and B, indicating the upflow that drives the conductive heating of high-porosity sediments may be associated with this fault. The fault is coring an anticline with a down-dropped stratigraphic section to the southwest which may explain the presence of deeper stratigraphic feed zones in this part of the field.

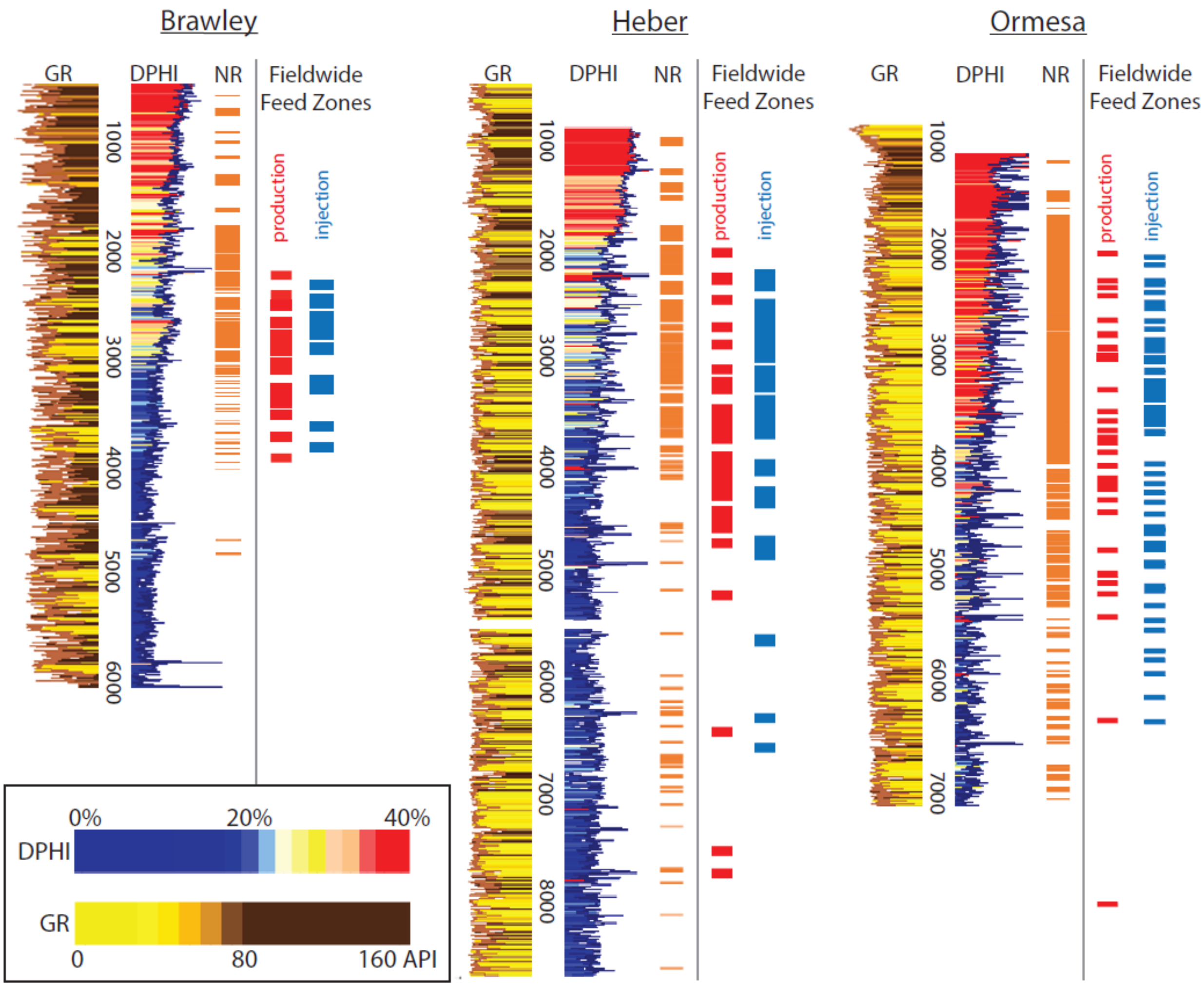

Figure 8: Gamma Ray (GR), Density-Porosity (DPHI), and calculated Net Reservoir (NR) for type logs from Brawley, Heber, and Ormesa geothermal fields. Fieldwide production and injection feed zones are displayed for each field to indicate the general depth ranges that are utilized for development.

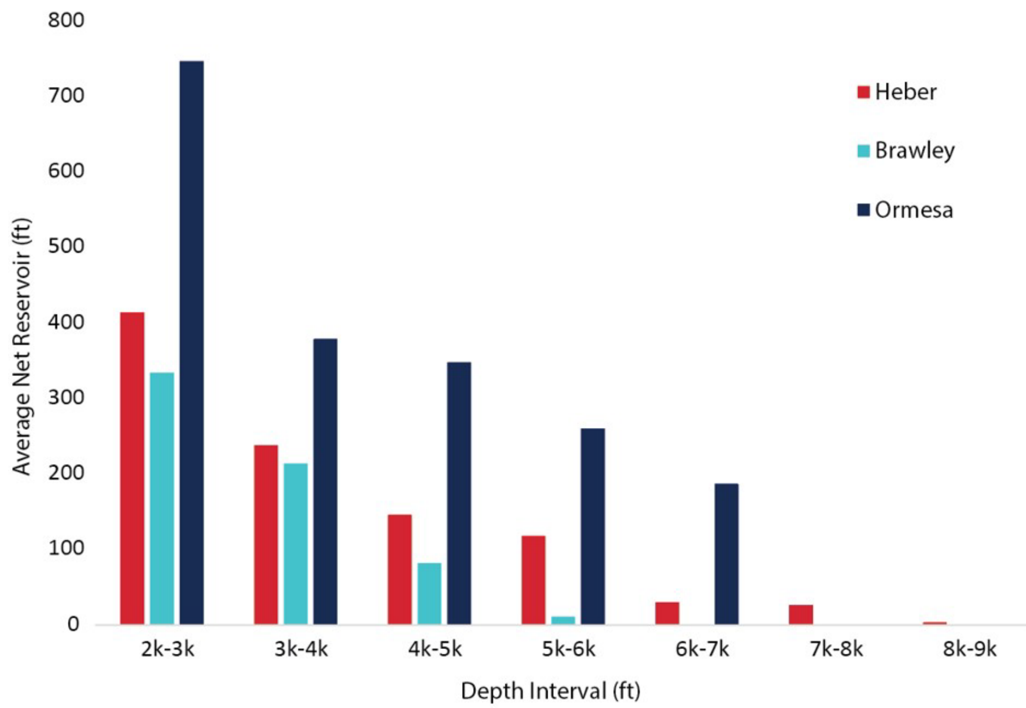

Figure 9: Average Net Reservoir calculated from multiple wells from each Ormat-operated field versus depth interval. Ormesa has the highest net reservoir and this is consistent with the field's proximity to the source of Colorado River-derived sediments. Brawley has the lowest net reservoir most likely due to a greater degree of low-porosity sediments from lacustrine deposition. Compared to Brawley, Heber has more net reservoir and a less rapid decline in net reservoir with depth.

6. Conceptual Models

Conceptual models for geothermal resources integrate geologic, geochemical, and geophysical data to visualize subsurface temperature and permeability distribution. This data is used to make informed decisions for well targeting and reservoir management. The conceptual models for the Heber, Brawley, and Ormesa are data-driven and highlight key similarities and differences in matrix and fracture permeability distribution, temperature, and intervals of productivity. Generating capacity and the median productivity index are key values to understand how the characteristics of each field influence productivity. Productivity index (P.I.) is a measure of the ability of a well to flow and is calculated by dividing the volumetric flow rate by the pressure drawdown in the wellbore at reservoir conditions (Grant and Bixley, 2011). A higher median P.I. value generally results from higher permeability for a given field.

6.1 Brawley

Upflow of 500°F geothermal fluids is controlled by steeply dipping, NNE to ENE striking faults of the Brawley Fault Zone (Figure 10a). Permeability is matrix-dominated in the conductively heated feed zones produced by Ormat between 2000 and 4000ft and fracture-dominated in the deeper, convective upflow below 4000ft. Net reservoir increases from east to west and there is a large reduction below 4000ft. Brawley has lower net reservoir than Heber and Ormesa due to a greater amount of lacustrine deposition. Hypersaline fluids, similar to what is encountered in the Salton Sea Geothermal Field, are present in the hotter, deeper, fracture-dominated reservoir and present corrosion and scaling challenges. Therefore, Ormat's development strategy is focused on the shallower, lower temperature reservoir within the high permeability sedimentary sequences. Tracer studies have shown that some of these faults are conductive while others are partially sealing and impede fluid flow, such as the fault between North Brawley and East Brawley. For this reason, North Brawley and East Brawley have their own production and injection configurations. Geothermal fluids are capped by the clay-rich Borrego-Brawley Formations from surface to 2000ft depth, preventing natural flow to the surface. Brawley has the lowest generating capacity of the Ormat-operated fields in the Imperial Valley, 13 MW, and a median P.I. of 5 GPM/psi. This is most likely due to the lower amount of net reservoir compared to Heber and Ormesa due to increased lacustrine deposition consistent with its position towards the center of the basin.

6.2 Heber

Upflow of 360°F geothermal fluids is controlled by a steeply dipping, NNE striking fault zone (Figure 10b). An asymmetrical outflow plume emanates from the NNE fault to the west and northwest and this is an effect of increased net reservoir as well as regional groundwater movement in this direction. Feed zones from 2000 to 8000ft are primarily controlled by matrix permeability down to 4000ft depth and are a combination of matrix and fracture permeability below 4000ft. Heber has higher net reservoir with a milder reduction with depth compared to Brawley, most likely due to less lacustrine deposition. From surface to 2000ft deep, thick units of impermeable claystone in the Borrego-Brawley Formations cap the permeable reservoir and impede flow to the surface. The Heber field has higher temperatures at shallower depths and a more abrupt change in temperature gradients at the interface of the Borrego-Brawley and Palm Springs Formations compared to Brawley and Ormesa because the Heber fracture zone extends up to shallower depths. Heber has the highest generating capacity, 81 MW, and median P.I., 9 GPM/psi, of the Ormat-operated fields. This is most likely due to the high effective permeability in thick intervals of high porosity sands from 2000 to 4000ft and the dual matrix and fracture permeability of the field below 4000ft depth.

6.3 Ormesa

Upflow of greater than 380°F geothermal fluids is controlled by a NW striking fault that cores the central Ormesa anticline (Figure 10c). There is a broad outflow to the north most likely influenced by favorable reservoir quality in that direction. Permeability is matrix-dominated in the feed zones from 2000 to 6000ft depth. Ormesa has higher net reservoir than Heber and Brawley and the sands are coarser, angular, and poorly sorted, consistent with its position as the most proximal field to the source of Colorado River sedimentation. There is evidence for fractures related to a NW striking fault below 6000ft depth although these fractures have not been proven to be as permeable as the Heber fracture zone. Ormesa has the second highest generating capacity, 36 MW, and median P.I., 7 GPM/psi, of the Ormat-operated fields. Although Ormesa has higher net reservoir than Heber, the effective permeability may be lower due to the angularity and poor sorting of proximal Colorado River-derived sands.

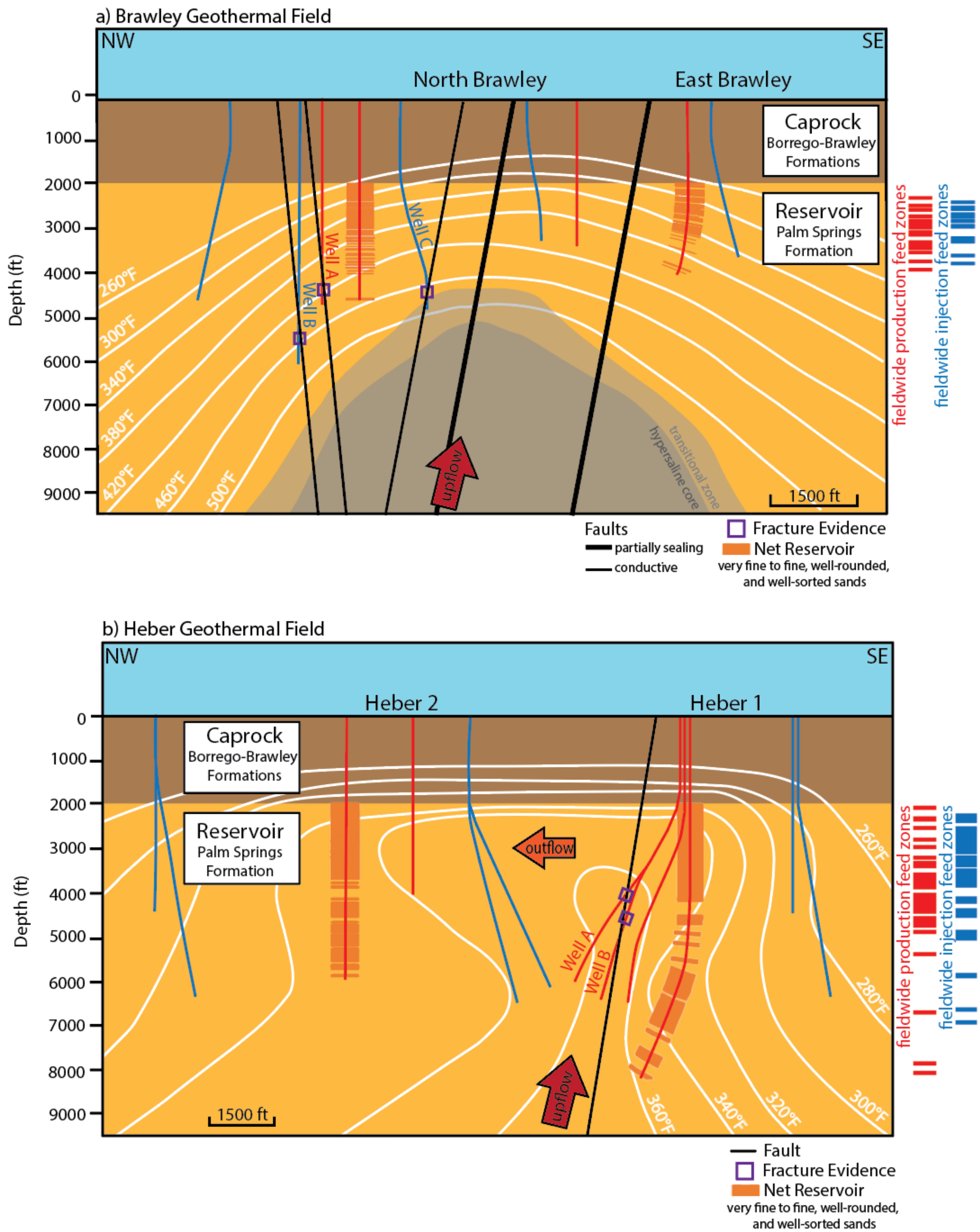
a) Brawley Geothermal Field
NW
SE
North Brawley
East Brawley
Depth (ft)
0
1000
2000
3000
4000
5000
6000
7000
8000
9000
Caprock
Borrego-Brawley
Formations
Reservoir
Palm Springs
Formation
Well A
Well B
Well C
260°F
300°F
340°F
380°F
420°F
460°F
500°F
upflow
transitional zone
hypersaline core
1500 ft
fieldwide production feed zones
fieldwide injection feed zones
Faults
partially sealing
conductive
Fracture Evidence
Net Reservoir
very fine to fine, well-rounded,
and well-sorted sands
b) Heber Geothermal Field
NW
SE
Heber 2
Heber 1
Depth (ft)
0
1000
2000
3000
4000
5000
6000
7000
8000
9000
Caprock
Borrego-Brawley
Formations
Reservoir
Palm Springs
Formation
outflow
Well A
Well B
upflow
260°F
280°F
300°F
320°F
340°F
360°F
1500 ft
fieldwide production feed zones
fieldwide injection feed zones
Fault
Fracture Evidence
Net Reservoir
very fine to fine, well-rounded,
and well-sorted sands

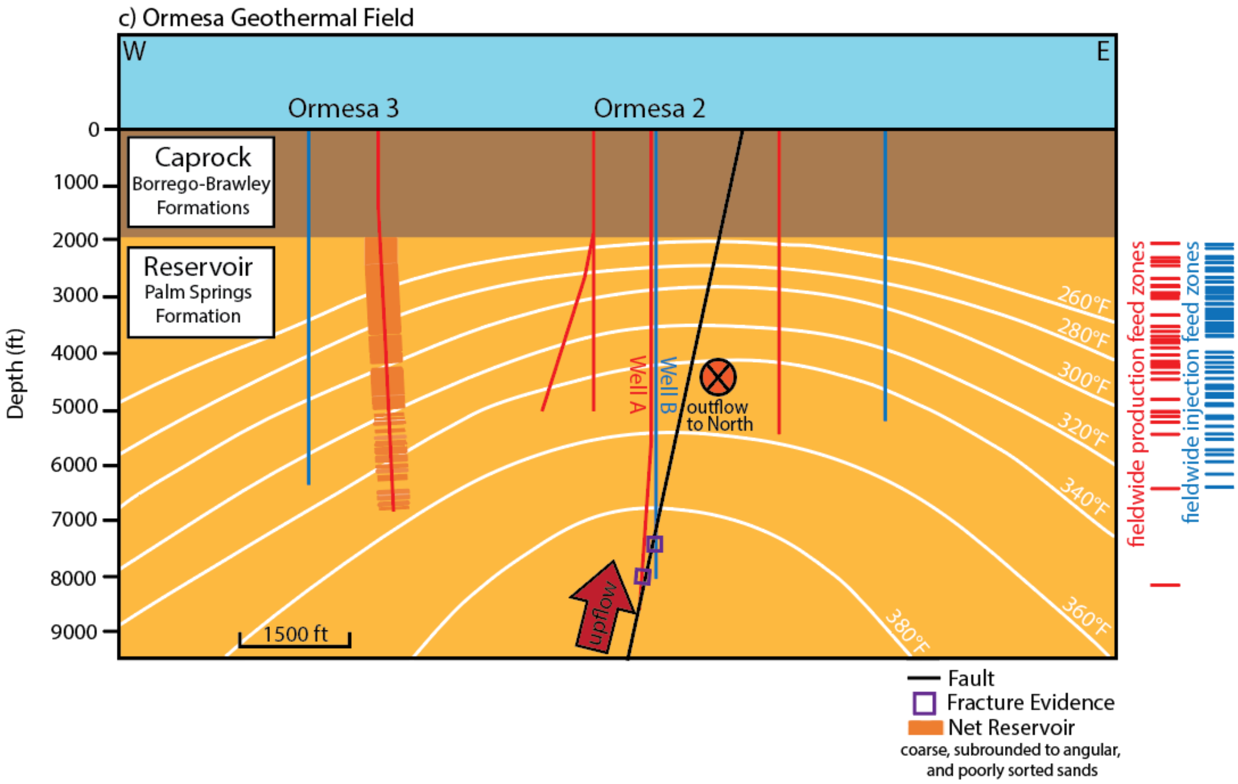

Figure 10: Conceptual models for a) Brawley, b) Heber, and c) Ormesa with upflow and outflow (if present), isotherms, major faults, locations of fracture evidence described in text, and production (red) and injection (blue) wells with net reservoir displayed on only a select number of wells for reference. Fieldwide production and injection feed zones are displayed for each to the right of the cross-section. Refer to text for full description.

7. Conclusions

The Salton Trough is an exemplary basin to study successful conventional geothermal development and operations. The anomalously high heat flow and thick sequences of clastic, high-porosity sediments at relatively shallow depths make the Trough an ideal geologic setting for geothermal development. The extensive generation history of these fields further demonstrates their sustainability. The use of binary technology and pumps contributes to the success of these low to moderate temperature systems. In this paper, we presented data-driven conceptual models for each of the Ormat-operated fields in Imperial Valley, CA through integrating data sets typical of oil and gas exploration and development (i.e., petrophysical logs and 2D/3D seismic). These conceptual models explore the temperature and permeability distributions at these systems as well as enable improved reservoir management decisions and allow for more predictable drilling results in the event of field expansions or well replacements.

Acknowledgement

The authors thank Ormat Technologies, Inc. for permission to publish this work.

REFERENCES

Anderson, T. “Geothermal Potential of Deep Sedimentary Basins in the United States.” *Unconventional Resources Technology Conference*, Denver, Colorado, USA (2013).

Ahmad, K., Kristaly, F., Turzo, Z., and Docs, R. “Effects of Clay Mineral and Physico-Chemical Variables on Sandstone Rock Permeability.” *Journal of Oil, Gas and Petrochemical Sciences,* (2011), 18-26.

Doe, B.R., Hedge, C.E., and White, D.E. 1966. “Preliminary Investigation of the Source of Lead and Strontium in Deep geothermal Brines Underlying the Salton Sea Geothermal Area.” Economic Geology, 61, (1966), 462-483.

Dorsey, R., Housen, B., Janecke, S., Fanning, M., and Spears, A. “Stratigraphic record of basin development within the San Andreas fault system: Late Cenozoic Fish Creek-Vallecito basin, southern California.” *GSA Bulletin*, 123, (2011), 771-793.

Elders, W. and Cohen, L. “The Salton Sea Geothermal Field, California, as a near-Field Natural Analog of a Radioactive Waste Repository in Salt.” *Technical Report, Office of Nuclear Waste Isolation*, Columbus, Ohio, 44, (1984), 565-572.

Elders, W.A., Combs, J., Coplen, T.B., Kolesar, P., and Bird, D.K. “Geophysical, Geochemical, and Geological Investigations of the Dunes Geothermal System, Imperial Valley, California.” *JPL Proc. of the Conf. on Res. for the Develop. of Geothermal Energy Resources*, Pasadena, California, (1974), 45-71.

Grant, M. and Bixley, P. “Well Completion and Heating.” *Geothermal Reservoir Engineering Second Edition,* (2011), 105-129.

Han, L., Hole, J., Stock, J., Fuis, G., Kell, A., Driscoll, N., Graham, K., Harding, A., Rymer, M., Gonzalez-Fernandez, A., and Lazaro-Mancilla, O. “Continental rupture and the creation of new crust in the Salton Trough rift, Southern California and northern Mexico: Results from the Salton Seismic Imaging Project.” *Journal of Geophysical Research: Solid Earth,* 121, (2016), 7469-7489.

Han, L., Hole, J., Stock, J., Fuis, G., Williams, C., Delph, J., Davenport, K., and Livers, A. “Seismic imaging of the metamorphism of young sediment into new crystalline crust in the actively rifting Imperial Valley, California.” *Geochemistry Geophysics Geosystems* (2016).

Kaspereit, D., Mann, M., Sanyal, S., Rickard, B., Osburn, W., and Hulen, J. “Updated conceptual model and reserve estimate for the Salton Sea geothermal field, Imperial Valley, California.” *Geothermal Resource Council Transactions*, 40, (2016), 57-66.

Kirby, S., Janecke, S., Dorsey, R., Housen, B., Langenheim, V., McDougall, K., and Steely, A. "Pleistocene Brawley and Ocotillo Formations: Evidence for Initial Strike-Slip Deformation along the San Felipe and San Jacinto Fault Zones, Southern California." The *Journal of Geology,* 115, (2007), 43-62.

Lippmann, M., Truesdell, A., and Fry, G. "The Cerro Prieto and Salton Sea Geothermal Fields- Are They Really Alike?" *Proceedings of the Twenty-Fourth Workshop on Geothermal Reservoir Engineering*, Stanford University, Stanford, CA, (1999).

Lonsdale, P. "Geology and tectonic history of the Gulf of California." *The Geology of North America: The Eastern Pacific Ocean and Hawaii,* (1989), 499-521.

Lutz, Andrew T. et al. "Stratigraphic Record of Pleistocene Faulting and Basin Evolution in the Borrego Badlands, San Jacinto Fault Zone, Southern California." *Geological Society of America Bulletin,* 118, (2006), 1377-1397.

Mazzini, A., Svensen, H., Etiope, G., Onderdonk, N., and Banks, D. "Fluid origin, gas fluxes and plumbing system in the sediment-hosted Salton Sea Geothermal System." *Journal of Volcanology and Geothermal Research*, 205, (2011), 67–83.

McKibben, M.A, Williams, A.E., and Okubo, S. "Metamorphosed Plio-Pleistocene evaporites and the origins of hypersaline brines in the Salton Sea geothermal System, California: Fluid Inclusion Evidence." *Geochimica et Cosmochimica Acta*, 52, (1988), 1047-1056.

Mooney, W., Laske, G., and Masters, T.G. "CRUST 5.1: a global crustal model at 5x5." *Journal of Geophysical Research: Solid Earth,* 103, 727-747.

Rex, R.W. "Origin of the Salt of the Imperial Valley an Surrounding Watershed Area." *Cooperative Investigation of Geothermal Resources in the Imperial Valley Area and their Potential Value for Desalting of Water and Other Purposes, Final Report, Contract No. 14-06-300-294, U.S. Department of the Interior, Bureau of Reclamation* (1972).

Rex, R.W. "The origin of the Brines of the Imperial Valley, California." *Geothermal Resources Council Transactions, Annual Meeting* (1983).

Sass, J., Galanis, S., Lachenbruch, A., Marshall, B., and Munroe, R. "Temperature, thermal conductivity, heat flow, and radiogenic heat production from unconsolidated sediments of the Imperial Valley, California." *USGS Report,* (1984).

Wallis, I., Rowland, J., Cumming, W., and Dempsey, D. "The Subsurface Geometry of a Natural Geothermal Reservoir." *New Zealand Geothermal Workshop,* Rotorua, New Zealand (2016).

White, D.E., 1981. "Active Geothermal Systems and Hydrothermal Ore Deposits." *Economic Geology, Seventy-Fifth Anniversary Volume*, (1981), 392-423.

Williams, A.E. and McKibben, M.A. "A brine interface in the Salton Sea Geothermal System, California: Fluid geochemical and isotopic characteristics." *Geochimica et Cosmochimica Acta,* 53, (1989), 1905-1920.